

# The ATLAS Pixel Detector

Jörn Grosse-Knetter<sup>a</sup>,  
on behalf of the ATLAS Pixel collaboration

<sup>a</sup>*Physikalisches Institut, Universität Bonn, Nussallee 12, D-53115 Bonn, Germany*

---

## Abstract

The ATLAS Pixel Detector is the innermost layer of the ATLAS tracking system and will contribute significantly to the ATLAS track and vertex reconstruction. The detector consists of identical sensor-chip-hybrid modules, arranged in three barrels in the centre and three disks on either side for the forward region.

The position of the Pixel Detector near the interaction point requires excellent radiation hardness, mechanical and thermal robustness, good long-term stability, all combined with a low material budget. The detector layout, results from final prototyping and the status of production are presented.

*Key words:* silicon detector, pixels, LHC

*PACS:* 06.60.Mr, 29.40.Gx

---

## 1 Introduction

The ATLAS Inner Detector [1] is designed for precision tracking of charged particles with 40 MHz bunch crossing identification. It combines tracking straw tubes in the outer transition-radiation tracker (TRT) and microstrip detectors of the semiconductor tracker (SCT) in the middle with the Pixel Detector, the crucial part for vertex reconstruction, as the innermost component.

The Pixel Detector [2] is subdivided

into three barrel layers in its centre, one of them around the beam pipe ( $r = 5$  cm), and three disks on either side for the forward direction. With a total length of approx. 1.3 m this results in a three-hit system for particles with  $|\eta| < 2.5$ .

The main components are approx. 1700 identical sensor-chip-hybrid modules, corresponding to a total of  $8 \cdot 10^7$  pixels. The modules have to be radiation hard to an ATLAS life time dose of 50 MRad or  $10^{15}$  neutron-equivalent.

---

*Email address:*  
jgross@physik.uni-bonn.de (Jörn Grosse-Knetter).

## 2 Module Layout

A pixel module consists of a single n-on-n silicon sensor, approx.  $2 \times 6 \text{ cm}^2$  in size. The sensor is subdivided into 47,268 pixels which are connected individually to 16 front-end (FE) chips via “bumps” [3]. These chips are connected to a module-control chip (MCC) [4] mounted on a kapton-flex-hybrid glued onto the back-side of the sensor. The MCC communicates with the off-detector electronics via opto-links, whereas power is fed into the chips via cables connected to the flex-hybrid.

To provide a high space-point resolution of approx.  $12 \mu\text{m}$  in azimuth ( $r\phi$ ), and approx.  $90 \mu\text{m}$  parallel to the LHC beam ( $z$ ), the sensor is subdivided into 41,984 “standard” pixels of  $50 \mu\text{m}$  in  $r\phi$  by  $400 \mu\text{m}$  in  $z$ , and 5284 “long” pixels of  $50 \times 600 \mu\text{m}^2$ . The long pixels are necessary to cover the gaps between adjacent front-end chips. The module has 46,080 read-out channels, which is smaller than the number of pixels because there is a  $200 \mu\text{m}$  gap in between FE chips on opposite sides of the module, and to get full coverage the last eight pixels at the gap must be connected to only four channels (“ganged” pixels). Thus on 5% of the surface the information has a two-fold ambiguity that will be resolved off-line.

The FE chips [3] contain 2880 individual charge sensitive analogue circuits with a digital read-out that operates at 40 MHz clock. The analogue part consists of a high-gain, fast preamplifier followed by a DC-

coupled second stage and a differential discriminator. The threshold of the discriminator ranges up to 1 fC, its nominal value being 0.5 fC. When a hit is detected by the discriminator the pixel address is provided together with the time over threshold (ToT) information which allows reconstruction of the charge seen by the preamplifier.

## 3 Module Prototypes

Several ten prototype modules have been built with a first generation of radiation-hard chips in  $0.25 \mu\text{m}$ -technology. In order to assure full functionality of the modules in the later experiment, measurements at the production sites, after irradiation, and in a test beam are performed.

### 3.1 *Laboratory measurements*

An important test that allows a large range of in-laboratory measurements is the threshold scan. Signals are created with on-module charge injection and scanning the number of hits versus the so injected charge yields the physical value of the threshold of the discriminator and the equivalent noise charge as seen by the preamplifier. A set of such scans is used to reduce the threshold dispersion by adjusting a DAC-parameter individually for each channel. The resulting threshold and noise after threshold tuning is shown in figure 1. Typically approx. 100 e threshold dispersion

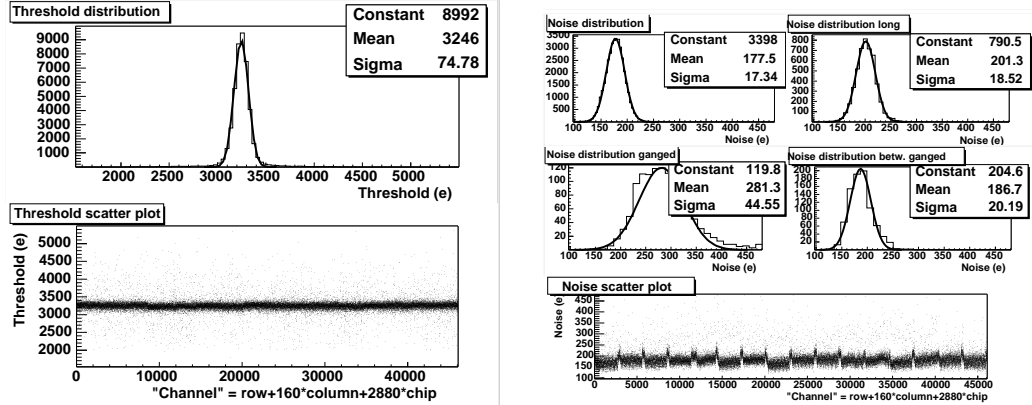


Fig. 1. Distributions of threshold (left) and noise (right) of a module after individual threshold tuning.

across a module and a noise value of below 200 e for standard pixels is achieved, as is needed for good performance. In a similar fashion, the cross-talk is measured to a few per cent for standard  $50 \times 400 \mu\text{m}^2$  pixels.

A measurement of the timewalk, i.e. the variation in the time when the discriminator input goes above threshold, is an issue since hits with a low deposited charge have an arrival time later than those with high charges, in particular for ganged pixels.

Data taken when illuminating the sensor with a radioactive source allows in-laboratory detection of defective channels. The source-spectrum reconstructed from the ToT-readings is in agreement with expectations.

### 3.2 Irradiation

Some of the prototype modules have been irradiated to a dose of 50 MRad,

approx. the dose expected after 10 years of ATLAS operation. The radiation damage is monitored reading the leakage current individually for each pixel. The single event upset rate is measured during irradiation.

The threshold dispersion and the noise after irradiation as shown in figure 2 is only modestly increased and still well in agreement with requirements for operation in ATLAS.

### 3.3 Test beam measurements

Tests have been performed in the beam line of the SPS at CERN using 180 GeV/c hadrons. The setup consists of a beam telescope for the position measurement [5], trigger scintillators for timing measurement to 36 ps, and up to four pixel modules. The number of defective channels is observed to less than  $10^{-3}$  and for standard  $50 \times 400 \mu\text{m}^2$  pixels the efficiency for normal incidence particles is  $99.57 \pm 0.15\%$ . The timewalk is measured to values similar to those from lab tests (see above).

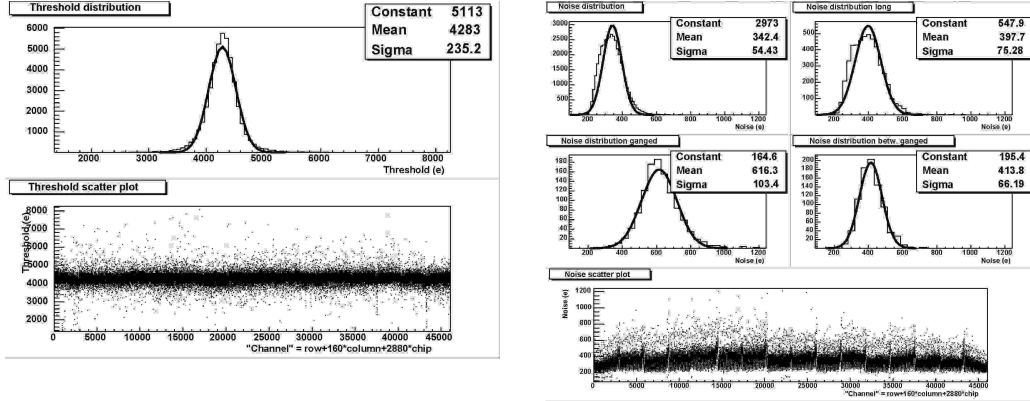


Fig. 2. Distribution of threshold (left) and noise (right) of a module after irradiation with 50 MRad.

Modules irradiated as described in section 3.2 have been tested in the beam line and the bias voltage needed for full depletion is measured to be between 500 and 600 V, see figure 3. The deposited charge is measured via the ToT readings and no significant changes in the uniformity w.r.t. unirradiated modules are observed.

### 3.4 Next generation of chips

The results of the prototype modules show that the chips fulfil largely the requirements of electrical performance and radiation hardness and that the production process has a high yield. Problems such as time-

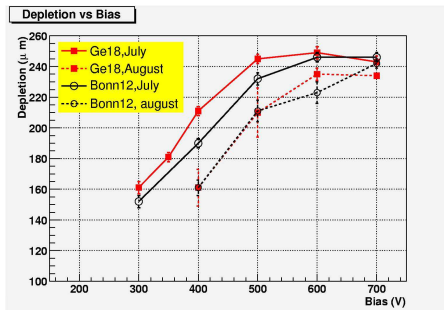


Fig. 3. Depletion depth measured in a test beam as a function of bias voltage.

walk and too little SEU tolerance have been addressed and solved in a new design of FE and MCC chips [3].

## 4 Off-detector electronics

The off-detector readout electronics is designed to process data at a rate of up to 100 kHz level-1 triggers. The main data-processing component is the “read-out driver” (ROD), of which first prototypes have been built to pixel specifications and are being evaluated. The first-step event-building and error flagging is done via FPGAs. The communication to the rest of the DAQ-system is run through a 1.6 Gbit/s opto-link. The communication to modules, online monitoring and calibration runs are performed with SRAMs and DSPs; their programming is ongoing and modules have already been configured and operated successfully with a ROD.

## 5 System aspects

### 5.1 Support structures

The mechanics of the system has to guarantee good positional stability of the modules during operation while the amount of material has to be kept to a minimum. At the same time it has to provide cooling to remove the heat load from the modules and maintain the sensors at a temperature of  $-6^{\circ}\text{C}$  to keep the radiation damage low.

Barrel-modules are glued to “staves”, long, flat carbon-structures with cooling pipes embedded. The staves are mounted inside halfshells, which themselves are assembled into frames to form the barrel system.

The disks are assembled from carbon-sectors with embedded cooling covering 1/12 of a wheel. The modules are glued directly to either side of the disk sectors.

### 5.2 Systemtests

First mini-systemtests have been performed with six modules on a disk sector and three modules on a barrel-stave. The noise behaviour on the disks or staves shows no significant differences compared to similar measurements with the same modules individually, see figure 4. Larger systemtests are already in preparation and will include realistic powering and read-out.

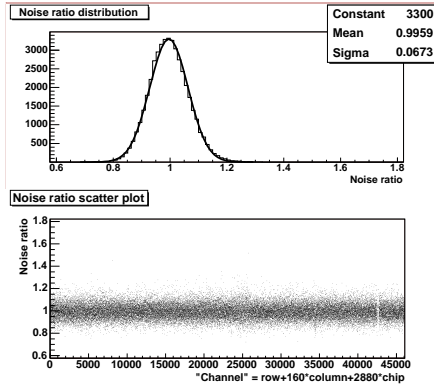


Fig. 4. Ratio of noise on one module comparing between simultaneous operation with two other modules and individual operation.

## 6 Conclusions

Prototype modules built with a first generation of radiation hard chips show largely satisfying performance in laboratory-test, in test beam studies and after irradiation. Remaining problems have been solved in a new generation of chips which is now ready for production.

Work on the off-detector electronics and the support structures have been going on in parallel and are well on track. First systemtest results are promising.

## References

- [1] Technical Design Report of the ATLAS Inner Detector, CERN/LHCC/97-16 and CERN/LHCC/97-17 (1997).
- [2] Technical Design Report of the ATLAS Pixel Detector, CERN/LHCC/98-13 (1998).
- [3] F. Hügging, this proceedings.

[4] R. Beccherle et al., Nuclear Instr.  
Meth. A **492**, 117 (2002).

[5] J. Treis et al., Nuclear Instr. Meth.  
A **490**, 112 (2002).